7th Australian Conference on Laser Diagnostics in Fluid Mechanics and Combustion
Melbourne, Australia
9-11 December 2015

Back-Illumination Imaging of Pressurised Metered-Dose Inhaler Sprays

N. Mason-Smith[1], D. Duke[2], M. Fedrizzi[1], J. Soria[1,3], D. Edgington-Mitchell[1] & D. Honnery[1]

[1]Department of Mechanical and Aerospace Engineering
Monash University, Clayton, Victoria, Australia

[2]Energy Systems Division
Argonne National Laboratory, Illinois, USA

[3]Department of Aeronautical Engineering
King Abdulaziz University, Jeddah, Kingdom of Saudi Arabia

Abstract

Sprays in the near-nozzle region of a pMDI are imaged with high spatial resolution back-illumination imaging to aid interpretation of laser extinction signals. Spray density varies continuously throughout the spray event, and between events, for all formulations studied. Spray widths increase until approximately 50 ms after the start of injection, after which the spray narrows until the metering chamber is depleted. Fluctuations in optical depth are reduced by the inclusion of ethanol, which reduces fluctuations in spray spread. In addition to many small droplets, visualisations show dense droplet clusters and large droplets.

Introduction

Pressurised metered-dose inhalers (pMDI) are used for the delivery of drugs for the treatment of asthma and other respiratory diseases. The spray developed is the result of a high vapour pressure propellant forcing a metered dose of drug-containing solution through an atomising nozzle. Cosolvents such as ethanol are commonly included to aid with drug solubility. Drug particle sizes are related to the initial droplet sizes, from which the propellant and cosolvent evaporate, by the drug concentration [16]. Typical pMDIs have small 50 µL metering chambers that isolate a volume of formulation from the canister. After actuation, the formulation flows from the metering chamber through an expansion chamber and discharges from an atomising nozzle. The pressure and temperature in the metering chamber decrease during injection [13], and injection ends when the metering chamber is depleted of formulation. Spray durations are on the order of 100 ms.

Many of the sprayed droplets have high velocities and large aerodynamic diameters, and as such are poor flow tracers that do not follow the user's comparatively slow inhalation. This results in a substantial deposition of drug in the mouth [4]. Prior studies have extensively characterised mean velocity and spreading characteristics of pMDI sprays [3, 5, 14], and there have also been observations of large fluctuations in cone angle and spray density, visualised in the near-nozzle region [5, 17] and downstream [12]. These large fluctuations in cone angle and spray density are expected to affect drug deposition *in vivo*, particularly if the droplets ejected during these events are poor tracers.

Line-of-sight optical techniques yield information on the path-integrated spray density, and with adequate temporal resolution can provide information on fluctuations in nozzle discharge. The non-dimensional optical depth τ [15], also known as the optical density [2] is related to the transmission $T = \left(\frac{I}{I_0}\right)$ by the Beer-Lambert law:

$$\tau = -\ln\left(\frac{I}{I_0}\right) \tag{1}$$

where I is the detected flux and I_0 is the incident flux in the absence of spray.

Extinction of a laser sheet oriented through the centreline of a spray downstream of the mouthpiece of a pMDI analogue [14] showed axially-convecting fluctuations in transmission, and these were interpreted as indicative of spray unsteadiness. These fluctuations in transmission were found to be reduced by the inclusion of ethanol in the formulation, which was interpreted as indicating a higher level of unsteadiness in propellant-only sprays. However, this interpretation is based on limited information, as fluctuations in optical depth may have several sources. Full-field back-illumination imaging is a technique that can complement laser extinction and assist with signal interpretation. In this paper, we investigate the near-nozzle region of sprays from metered-dose inhalers with high spatial resolution back-illumination imaging. The obtained dataset is a complementary measure of near-nozzle spray structure, and assists the interpretation of line and point measurements of pMDI sprays. Due to the difficulty of obtaining full-field images with adequate temporal resolution, high sample-rate laser extinction remains an attractive technique for study of the time-variant spray density.

Experimental Methodology

Spray Apparatus

A linear solenoid-driven pMDI actuator was developed [1] and was used to generate sprays from metered-dose inhalers [14]. A Bespak inhaler body was used with the mouthpiece removed to allow imaging of the near-nozzle region (Figure 1). The nozzle exit is recessed in a bowl and located 3mm upstream of the coordinate system (Figure 1). Metered canisters containing propellants HFA 134a and HFA 227, with and without ethanol, were used to generate drug-free sprays. Canister metering valves were 50 µL. Inhaler body and canister dimensions are given in Table 1; the reader is referred to [9] for the significance of each dimension. Formulations used are shown in Table 2, specifying weight fractions of each constituent.

Back-Illumination Imaging

A back-illumination imaging setup was used to visualise the spray in the near-nozzle region. Illumination was provided by a strobed Phlatlight CBT-120 LED. Short pulse durations and low duty cycles allowed a current several times higher than the safe continuous rating to be used [20]. This greatly increased the lu-

Dimension	Size (mm)
Nozzle orifice diameter (d_{no})	0.3
Nozzle orifice length (l_{no})	0.6
Valve stem diameter, inner ($d_{vs,i}$)	2.0
Valve stem diameter, outer ($d_{vs,o}$)	3.2
Valve stem length (l_{vs})	12
Valve orifice diameter (d_{vo})	0.6

Table 1: Canister and nozzle dimensions.

Formulation	% HFA134a	% HFA227	% EtOH
134a	100	0	0
227	0	100	0
134a-E	85	0	15
227-E	0	85	15

Table 2: Canister formulations, composition by weight of propellant (HFA134a and HFA227) and ethanol (EtOH).

minous flux during imaging. A guide to safe operation of these LEDs for high-speed imaging is given in [18]. To minimise the light pulse duration, imaging was performed without a diffuser to maximise the luminous flux. However, the LED pulse duration of 100 ns is inadequate to image the fastest droplets without motion blur.

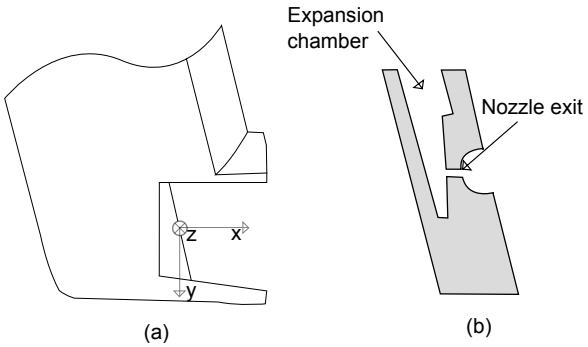

Figure 1: Schematic of (a) Bespak inhaler body with mouthpiece removed, allowing visualisation of the near-nozzle region; and (b) nozzle internal geometry.

A PCO Dimax was used to acquire image sequences of ≥ 40 spray events for each formulation. High magnification was achieved with a Nikon 105mm lens, a bellows and a 25mm macro tube. Image acquisition parameters are given in Table 3. The camera's double-shutter function was used, and the recorded image pairs can be used for "shadowgraph PIV" [7, 19]. Two-point radiometric calibration was used to correct for inhomogeneous back-illumination and the sensor's (albeit very low) fixed pattern noise [10]. Results are presented in regions where the reference intensity was sufficient to measure transmission with a minimum of 10-bit radiometric resolution. A BeagleBone Black programmable pulse generator [8] was used to trigger the experiment.

Results and Discussion

To characterise the mean spray structure, transverse profiles of optical depth were obtained by ensemble averaging. The temporal evolution of ensemble-average (≥ 40 spray events) radial profiles of optical depth at x = 2 mm are presented in Figure 2. Spray half-widths, defined by the half-width half-maximum (HWHM) of optical depth, are shown as isolines on the temporal evolution plot.

Parameter	Value
Frame rate (image pairs/s)	500
Interpulse time (µs)	4
Light pulse duration (ns)	100
Magnification (pixels/mm)	307
Magnification factor	3.4
Radiometric resolution (bits/pixel)	12

Table 3: Back-illumination imaging parameters.

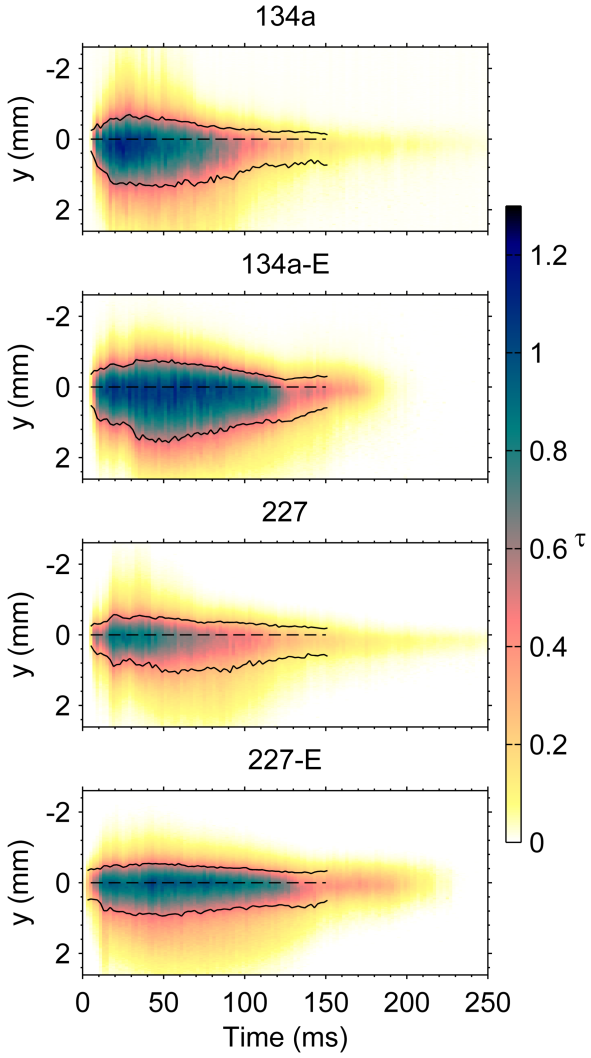

Figure 2: Temporal evolution of ensemble average transverse profile at x = 2 mm. Spray axes (black dashed lines) and spray half-widths (black solid lines) are overlaid.

Spray transience is observable–optical depth peaks around 25-50 ms after start of injection for all formulations, after which it decays. Discharge profiles differ for propellant-only and ethanol-containing formulations. A long time is required for the optical depth to reach zero on the centreline for propellant-only formulations, suggesting there is a long discharge. Ethanol-containing formulations cease more rapidly, though have a sustained period of high and nominally constant centreline optical depth. All formulations have high radial gradients of optical depth at x = 2 mm, exceeding 1 mm^{-1}. Axial gradients are

lower, on the order of 0.1 mm^{-1}. Profiles are also visibly asymmetric about the centreline, with a greater optical depth through the spray event located below the spray axis.

The observed asymmetry of the spray profiles in Figure 2 is investigated by measuring spray widths, providing a local measure of the extent of the spray. Spray half-widths are plotted in Figure 3. Half-widths are antisymmetric about the spray axis, and the spray is widest below the spray axis. With reference to the nozzle internal geometry (Figure 1), the wider spray occurs below the nozzle orifice. Formulation is also seen to affect the spray width, as HFA134a sprays are wider in the mean than those propelled by HFA227.

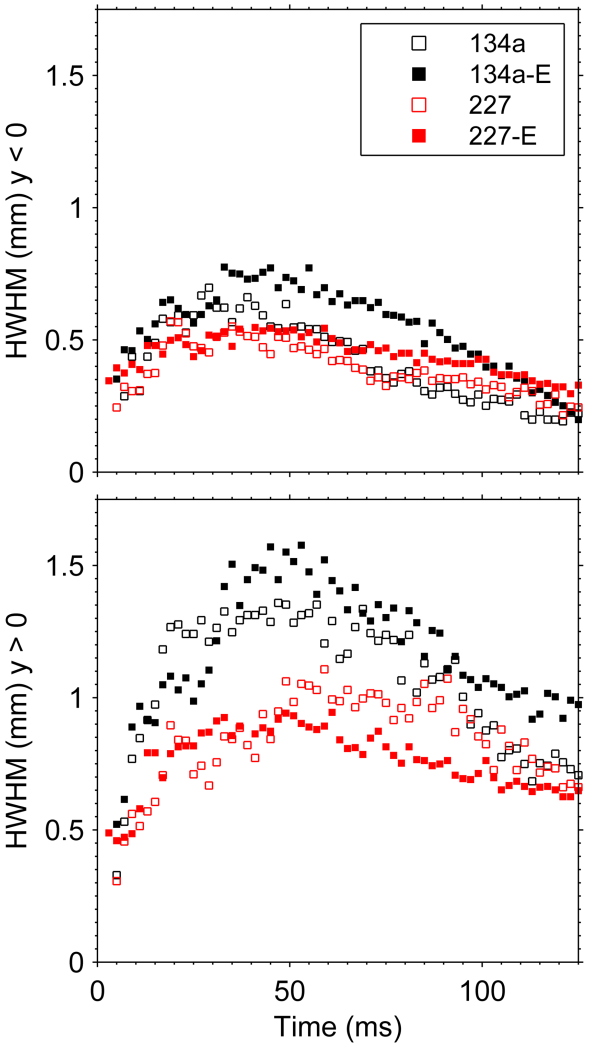

Figure 3: Ensemble-average spray half-widths at x = 2 mm, above and below the spray axis.

Importantly, the transverse profiles also depict spray discharge characteristics that may be misinterpreted with a point measurement. Ethanol-containing formulations have a period of almost constant optical depth along the spray axis for 25-100 ms after the start of injection. Taken in isolation, this would suggest the presence of a steady state, however the spray width varies continuously over this period and narrows after it peaks at around 50 ms (Figure 3). For the formulations and metering volume studied, pMDI sprays exhibit no steady-state.

In addition to a transient spray density that results from metered discharge, pMDI sprays exhibit a high degree of interspray variability. This is illustrated with the time evolution of a profile ensemble RMS, shown in Figure 4. RMS profiles are generated at x = 2 mm from $\geq$ 40 spray events. Spatial binning of 1 nozzle diameter in x was used to increase the number of samples used to calculate the RMS, however as the samples are not independent there remains a large uncertainty on the resulting plot.

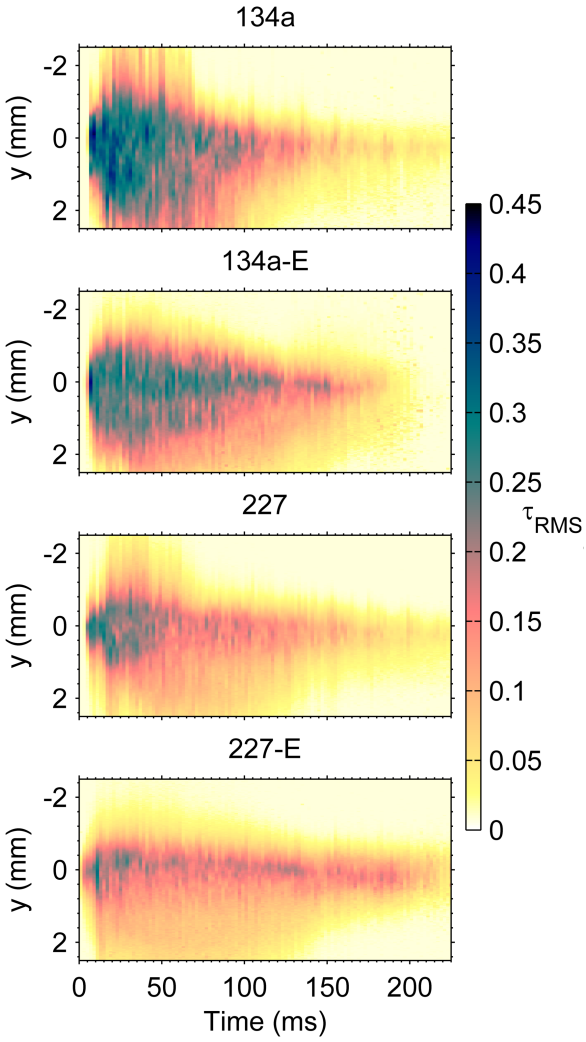

Figure 4: Temporal evolution of transverse profile RMS at x = 2 mm.

Fluctuations in optical depth are highest for 134a-propelled sprays. For both propellants, fluctuations in optical depth are reduced by the inclusion of ethanol. The lowest magnitude of fluctuations was seen with 227-E, which represents the lowest vapour pressure formulation studied [14].

Instantaneous images are presented to illustrate the sources of fluctuations. Instantaneous images of 134a sprays 50 ms after start of injection are shown in Figure 5. Though imaged at the same time after start of injection, the spray structures vary considerably. In the top image, the spray appears concentrated on the centreline. Some droplet clusters are seen, and there is very little spray visualised above the spray axis. In the lower image, a large number of droplets are present above and below the spray axis, and their trajectory relative to the spray axis indicates a significant increase in the instantaneous cone angle. The overall spray density is also substantially increased. This large variability in spray density may be related to a two-phase flow

instability driven by propellant boiling in the nozzle. The spray appears finely atomised for both images.

Propellant-only sprays of HFA227 at this same time are shown in Figure 6. The spray is finely atomised in the upper image, and has a low optical density as is expected from the mean profiles (Figure 2). The lower image shows a 'shedding' event in which a mass of liquid emerges from the nozzle as large droplets. These droplets are unlikely to trace the user's breath and would be expected to substantially contribute to deposition of drug in the mouth.

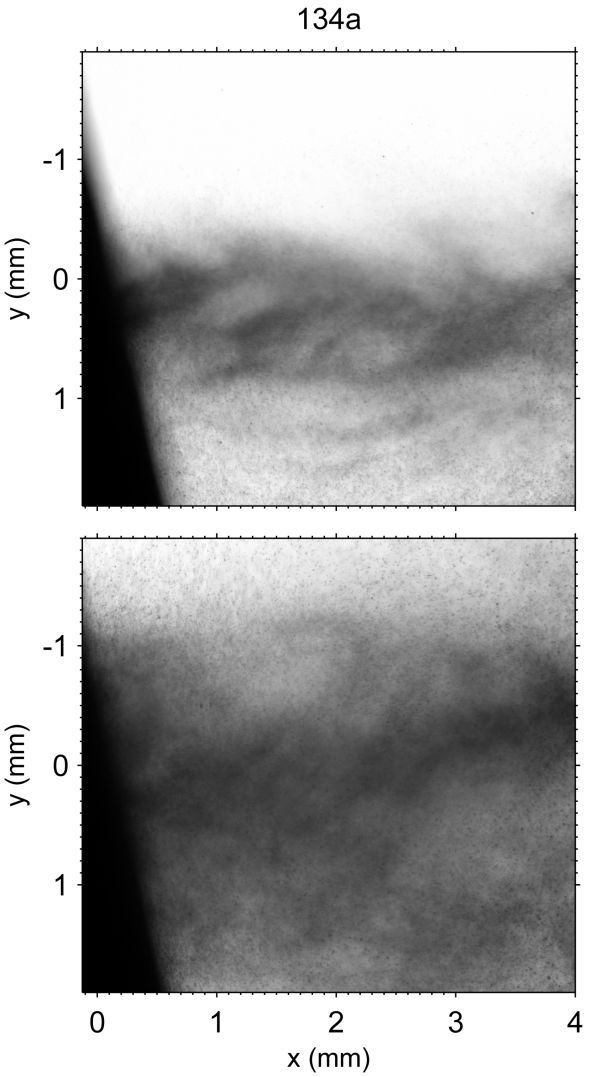

Figure 5: Instantaneous back-illumination spray images of near-nozzle region for independent 134a spray events, both imaged 50 ms after start of injection.

Instantaneous image sets show that the inclusion of ethanol alters spray morphology for both propellants, and spreading rate fluctuations are reduced. For 134a-E, RMS optical depth is high, and these fluctuations are the product of a local variability in structure that convects through the spray region. The 134a-E sprays are wider in the mean than 134a (Figure 3), and instantaneous images (Figure 7, top) show that this increased width is consistent. Substantial groups of droplet clusters are present in the sprays, and there is spray present both above and below the spray axis. 227-E sprays similarly did not fluctuate substantially in spread. As per the propellant-only case, 227-E spray images showed the presence of many large droplets that would be unlikely to be respirable.

Unsteadiness as measured in the framework of Edwards and Marx [6] is highest at the periphery of two-phase effervescent sprays [11]. Centreline optical depths vary substantially less relative to the mean than the optical depths at the spray periphery. Laser line extinction measurements intended to characterise spray unsteadiness for pMDIs are likely to obtain a stronger signal in regions at the periphery of pMDI sprays, rather than along the spray axis [14].

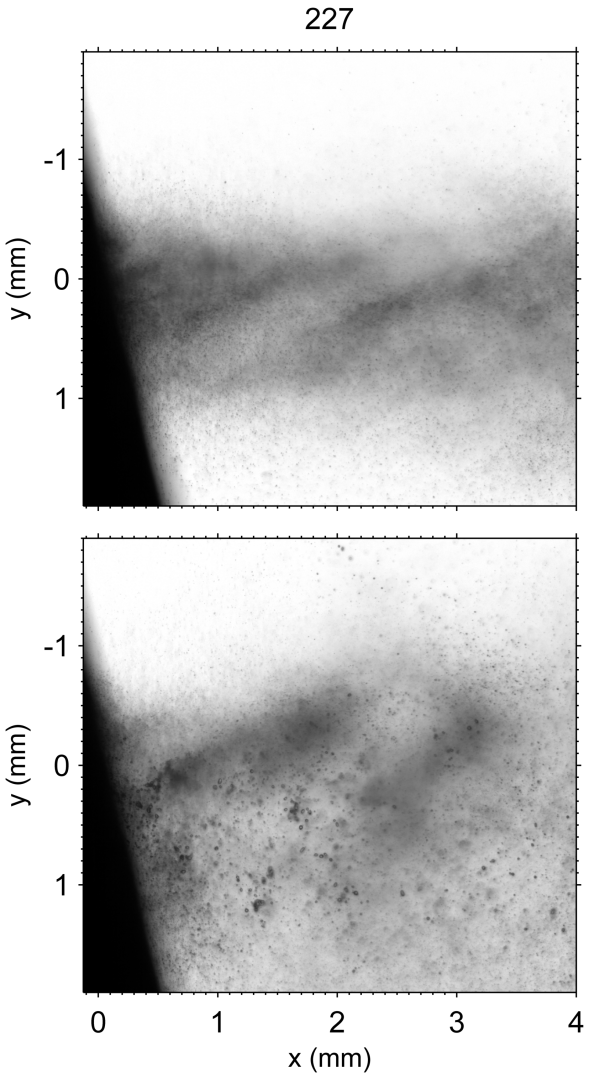

Figure 6: Instantaneous back-illumination spray images of near-nozzle region for independent 227 spray events, both imaged 50 ms after start of injection.

Conclusions

Back-illuminated images of sprays from pMDIs were collected in the near-nozzle region. Spray density was observed to vary throughout the injection, which is entirely transient. Sprays are asymmetric about the spray axis in the near-nozzle region. Fluctuations in optical depth are highest for 134a-propelled sprays, and for both propellants the fluctuations are reduced by the inclusion of ethanol. Propellant-only sprays exhibit large fluctuations in cone angle, whereas ethanol-containing sprays exhibit large fluctuations in local spray density with less substantial

fluctuations in spread. Formulations with propellant 227 discharged substantial masses of liquid as large droplets.

Acknowledgements

The authors gratefully acknowledge the support given to the project by the Australian Research Council.

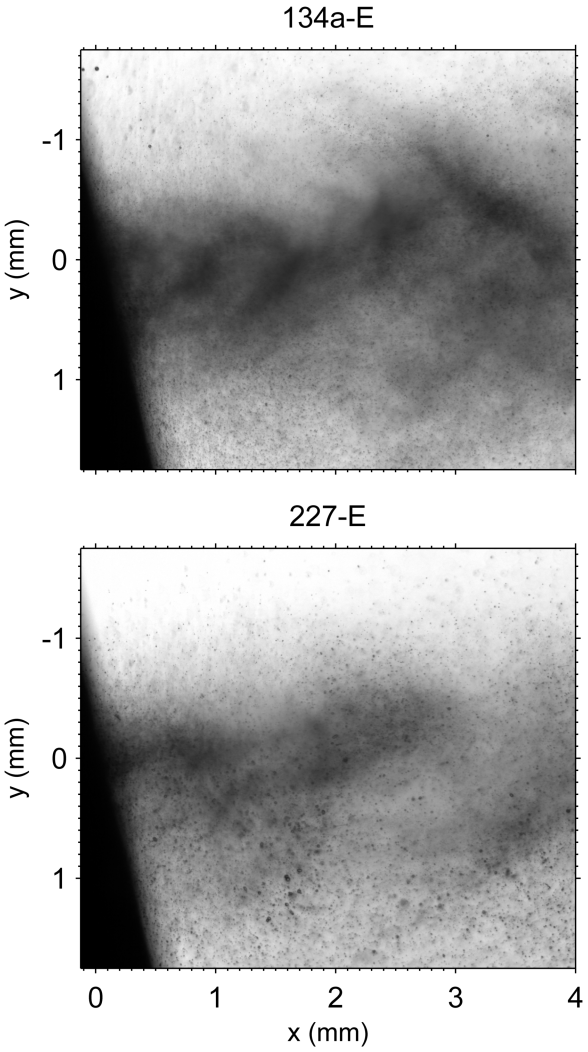

Figure 7: Instantaneous back-illumination spray images of near-nozzle region for (top) 134a-E and (bottom) 227-E sprays, both imaged 50 ms after start of injection.

References

[1] N. A. Buchmann, D. J. Duke, S. A. Shakiba, D. M. Mitchell, P. J. Stewart, D. Traini, P. M. Young, D. A. Lewis, J. Soria, and D. Honnery, "A novel high-speed imaging technique to predict the macroscopic spray characteristics of solution based pressurised metered dose inhalers," *Pharmaceutical research*, vol. 31, no. 11, pp. 2963–2974, 2014.

[2] N. Chigier, "Optical imaging of sprays," *Progress in Energy and Combustion Science*, vol. 17, no. 3, pp. 211–262, 1991.

[3] B. M. Crosland, M. R. Johnson, and E. A. Matida, "Characterization of the spray velocities from a pressurized metered-dose inhaler," *Journal of aerosol medicine and pulmonary drug delivery*, vol. 22, no. 2, pp. 85–98, 2009.

[4] R. Dhand, "Aerosol plumes: Slow and steady wins the race," *Journal of Aerosol Medicine*, vol. 18, no. 3, pp. 261–263, 2005.

[5] C. Dunbar, A. Watkins, and J. Miller, "An experimental investigation of the spray issued from a pMDI using laser diagnostic techniques," *Journal of aerosol medicine*, vol. 10, no. 4, pp. 351–368, 1997.

[6] C. F. Edwards and K. Marx, "Multipoint statistical structure of the ideal spray, part II: Evaluating steadiness using the interparticle time distribution," *Atomization and Sprays*, vol. 5, no. 4&5, 1995.

[7] J. Estevadeordal and L. Goss, "PIV with LED: Particle shadow velocimetry (PSV)," in *43rd AIAA aerospace sciences meeting and exhibit, meeting papers*, 2005, pp. 12 355–12 364.

[8] M. Fedrizzi and J. Soria, "Application of a single-board computer as a low-cost pulse generator," *Measurement Science and Technology*, vol. 26, no. 9, p. 095 302, 2015.

[9] J. W. Ivey, R. Vehring, and W. H. Finlay, "Understanding pressurized metered dose inhaler performance," *Expert opinion on drug delivery*, pp. 1–16, 2014.

[10] B. Jähne, *Digital image processing, 6th ed.* Springer, 2005.

[11] J. Jedelsky and M. Jicha, "Unsteadiness in effervescent sprays: A new evaluation method and the influence of operational conditions," *Atomization and Sprays*, vol. 18, no. 1, 2008.

[12] D. Ju, J. Shrimpton, M. Bowdrey, and A. Hearn, "Effect of expansion chamber geometry on atomization and spray dispersion characters of a flashing mixture containing inerts. part II: High speed imaging measurements," *International journal of pharmaceutics*, vol. 432, no. 1, pp. 32–41, 2012.

[13] D. Ju, J. Shrimpton, and A. Hearn, "The effect of reduction of propellant mass fraction on the injection profile of metered dose inhalers," *International journal of pharmaceutics*, vol. 391, no. 1, pp. 221–229, 2010.

[14] N. Mason-Smith, D. Edgington-Mitchell, D. Honnery, D. Duke, and J. Soria, "Pressurised metered-dose inhaler spray structure," in *Proceedings of Turbulence and Shear Flow Phenomena 9*, Melbourne, Australia, 30 June - 3 July 2015.

[15] L. M. Pickett, J. Manin, A. Kastengren, and C. Powell, "Comparison of near-field structure and growth of a diesel spray using light-based optical microscopy and X-ray radiography," *SAE International Journal of Engines*, vol. 7, no. 2014-01-1412, pp. 1044–1053, 2014.

[16] S. W. Stein and P. B. Myrdal, "A theoretical and experimental analysis of formulation and device parameters affecting solution MDI size distributions," *Journal of pharmaceutical sciences*, vol. 93, no. 8, pp. 2158–2175, 2004.

[17] H. Versteeg, G. Hargrave, and M. Kirby, "Internal flow and near-orifice spray visualisations of a model phar-

maceutical pressurised metered dose inhaler," in *Journal of Physics: Conference Series*, IOP Publishing, vol. 45, 2006, p. 207.

[18] C. Willert, B. Stasicki, J. Klinner, and S. Moessner, "Pulsed operation of high-power light emitting diodes for imaging flow velocimetry," *Measurement Science and Technology*, vol. 21, no. 7, p. 075 402, 2010.

[19] C. Willert, S. Freitag, and C. Hassa, "High speed imaging of fuel spray using a low-cost illumination source," in *22nd European Conference on Liquid Atomization and Spray Systems (ILASS 2008), Como Lake, Italy, September*, 2008, pp. 8–10.

[20] C. E. Willert, D. M. Mitchell, and J. Soria, "An assessment of high-power light-emitting diodes for high frame rate schlieren imaging," *Experiments in fluids*, vol. 53, no. 2, pp. 413–421, 2012.